An *f-P/Q* Droop Control in Cascaded-Type Microgrid

Yao Sun, *Member, IEEE*, Guangze Shi, Xing Li, Wenbin Yuan, Mei Su, Hua Han, and Xiaochao Hou

***Abstract*—In cascaded-type microgrid, the synchronization and power balance of distributed generators become two new issues that needs to be addressed urgently. To that end, an *f-P/Q* droop control is proposed in this letter, and its stability is analyzed as well. This proposed droop control is capable to achieve power balance under both resistive-inductive and resistive-capacitive loads autonomously. Compared with the inverse power factor droop control, an obvious advantage consists in extending the scope of application. Finally, the feasibility of the proposed method is verified by simulation results.**

***Index Terms*—Cascaded-type microgrid, droop control, power balance.**

I. Introduction

MICROGRID offers an effective solution to reliably integrate distributed energy resources [1], which can operate in both grid-connected and islanded modes. The microgrid can be divided into two categories by its configuration: paralleled-type and cascaded-type ones. The former one has been intensively investigated [2]–[5]. The droop control is widely used to realize power sharing for paralleled-type microgrid [2], and extended into other applications which include the state-of-charge (SOC) balance for storage system [3], the optimal economical-sharing scheme of distributed generators (DGs) [4] and the droop control with MPPT of PV system [5]. However, the cascaded-type microgrid is a new one [6]–[10], which has only recently been presented.

The cascaded converter is originally applied to multilevel inverters [6], and initially extended into microgrid applications [7]–[10] for attaining higher voltage level and better utilization. Especially for PV grid-connected application [7] and battery management [8], the cascaded-type is very practical. In islanded cascaded-type microgrid, power balance among all modules is essential [9], [10]. An inverse droop control is firstly proposed to achieve power balance [9], which could also be used in DC microgrid. While for AC microgrid, an inverse power factor droop control is innovatively proposed to achieve power balance [10]. However, the method in [10] is only applicable to the cases of the resistive-inductive loads.

To overcome the limitation in [10], this letter proposes an *f-P/Q* droop control scheme in the cascaded-type microgrid. Frequency synchronization and power sharing among all DGs are achieved autonomously under both resistive-inductive and resistive-capacitive loads. The stability of the proposed scheme is proved theoretically.

Manuscript received March 7, 2017; revised June 9, 2017, July 23, 2017, and September 3, 2017; accepted September 6, 2017. Date of publication September 14, 2017; date of current version December 20, 2017. This work was supported in part by the National Natural Science Foundation of China under Grant 61573384, in part by the National Natural Science Foundation of China under Grant 61622311, and in part by the Natural Science Foundation of Hunan Province of China under Grant 2016JJ1019. Paper no. PESL-00038-2017. *(Corresponding author: Yao Sun.)*

Y. Sun, G. Shi, W. Yuan, M. Su, H. Han, and X. Hou are with the School of Information Science and Engineering, Central South University, Changsha 410083, China (e-mail: yaosuncsu@gmail.com; 16414986@qq.com; ywb_csu@163.com; sumeicsu@mail.csu.edu.cn; hua_han@126.com; houxc10@csu.edu.cn).

X. Li is with the College of Electrical and Information Engineering, Hunan University, Changsha 410082, China (e-mail: xingliaaa@gmail.com).

Color versions of one or more of the figures in this letter are available online at http://ieeexplore.ieee.org.

Digital Object Identifier 10.1109/TPWRS.2017.2752646

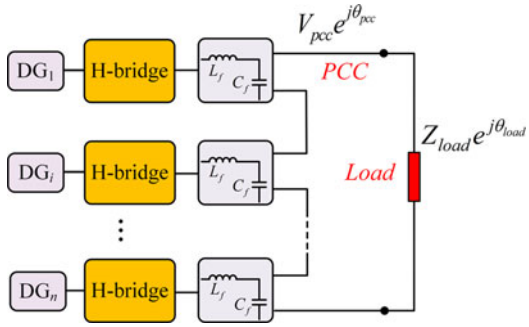

Fig. 1. Structure of islanded cascaded-type microgrid.

II. Analysis of Decentralized Power Balance Control

A. Equivalent Models of Islanded Cascaded-Type Microgrid

Fig. 1 shows the diagram of an islanded cascaded-type microgrid. These DG interfacing inverters are cascaded and supply power for loads together. The output real power P_i and reactive power Q_i of the *i-th* DG are derived as follows

$$P_i + jQ_i = V_i e^{j\theta_i} \cdot \left(V_{pcc} e^{j\theta_{pcc}} / |Z_{load}| e^{j\theta_{load}}\right)^* \tag{1}$$

where V_i and θ_i represent the output voltage amplitude and phase angle of the *i-th* DG. The ac bus voltage $V_{pcc}e^{j\theta_{pcc}}$ is the sum of the each DG voltage.

$$V_{pcc}e^{j\theta_{pcc}} = \sum_{i=1}^{n} V_i e^{j\theta_i} \tag{2}$$

According to (1)–(2), the power transmission characteristics of the *i-th* DG are obtained as

$$P_i = V_i \sum_{j=1}^{n} V_j \cos\left(\theta_i - \theta_j + \theta_{load}\right) / |Z_{load}| \tag{3}$$

$$Q_i = V_i \sum_{j=1}^{n} V_j \sin\left(\theta_i - \theta_j + \theta_{load}\right) / |Z_{load}| \tag{4}$$

where Z_{load} is the load impedance. The subscript j represents the serial number of the *j-th* DG.

B. Proposed f-P/Q Droop Control

To synchronize each DG in the cascaded-type microgrid without communication, a decentralized control scheme is designed as follow

$$\omega_i = \omega^* + m_i P_i / Q_i \tag{5}$$

$$V_i = V^* \tag{6}$$

where ω_i and V_i are the angular frequency and voltage amplitude references of the *i-th* DG, respectively. ω^* represents value of ω at no load. V^* is the nominal voltage value. Note that there is a singularity in (5) when $Q_i = 0$. To avoid the singularity and guarantee a reasonable frequency deviation, m_i is designed as follows.

$$m_i = \begin{cases} k_i Q_{\min}, & |Q_i| \geq Q_{\min} \\ k_i |Q_i|, & |Q_i| < Q_{\min} \end{cases} \tag{7}$$

where $Q_{\min}$ is a small positive constant, which is determined by practical requirements. k_i is a positive constant which is equal to $|\Delta\omega_{\max}/P^*_{\max\_i}|$. $\Delta\omega_{\max}$ is the allowable maximum frequency deviation and $P^*_{\max\_i}$ is the nominal rated power of the *i-th* DG.

For simplicity, we assume that the rated capacities of all DGs are same in steady state. Because the voltage amplitude references are same for all DGs and each DG shares the same load current, the apparent powers of all DGs are equal.

$$S_1 = S_2 = \cdots = S_n \tag{8}$$

For the purpose of power balance, let $k_i = K$; $i \in \{1, 2 \ldots \mathrm{n}\}$. Then (9) is derived from (5), (7) and (8).

$$P_1 = P_2 = \cdots = P_n \tag{9}$$

From aforementioned analysis, it could also be concluded that the phase angles of all DGs are the same. Therefore, it is easy to regulate the ac bus voltage by setting $V_i = V^*_{pcc}/n$, where V^*_{pcc} is the nominal voltage amplitude of the ac bus.

C. Small Signal Analysis

To prove the stability of the proposed method, the small signal analysis is used in this section [11]. First linearization is carried out [12]. The steps of linearization include: a) find the equilibrium points; b) move the equilibrium point to the origin; c) take the linearization of the system.

Since $\dot{\theta}_i = \omega_i$, the dynamic equation of the *i-th* DG is given by combining (3)–(6).

$$\dot{\theta}_i = \begin{cases} \omega^* + B_1 \dfrac{\sum_{j=1}^{n} \cos\left(\theta_i - \theta_j + \theta_{load}\right)}{\sum_{j=1}^{n} \sin\left(\theta_i - \theta_j + \theta_{load}\right)} |Q_i| \geq Q_{\min} \\ \omega^* + B_2 \sum_{j=1}^{n} \cos\left(\theta_i + \theta_{load} - \theta_j\right) |Q_i| < Q_{\min} \end{cases} \tag{10}$$

where $B_1 = K \cdot Q_{\min}; B_2 = KV^{*2}\mathrm{sgn}(Q_i)/|Z_{load}|$.

It is reasonable to assume the state variables in equilibrium point are $[\theta_{1s}, \theta_{2\,s} \ldots, \theta_{ns}]$, where $\theta_{is} = \omega_s t + \theta_{i0}, i \in \{1, 2 \ldots n\}$. ω_s is a steady state value of ω_i, and θ_{i0} depends on the selection of reference phase angle.

To move the equilibrium point to the origin, we take the transformation $\tilde{\theta}_i = \theta_i - \theta_{is}$. Then the small-signal equation of (10) is expressed as

$$\Delta\dot{\tilde{\theta}}_i = \begin{cases} -C_1 \sum_{j=1}^{n} \left(\Delta\tilde{\theta}_i - \Delta\tilde{\theta}_j\right) |Q_i| \geq Q_{\min} \\ -C_2 \sum_{j=1}^{n} \left(\Delta\tilde{\theta}_i - \Delta\tilde{\theta}_j\right) |Q_i| < Q_{\min} \end{cases} \tag{11}$$

where $C_1 = B_1/(n\sin^2\theta_{load})$, $C_2 = B_2 \cdot \sin\theta_{load}$ and Δ means a small perturbation around the steady state points.

Rewrite (11) in matrix form as

$$\Delta\dot{\tilde{\theta}} = \begin{cases} A_1 \cdot \Delta\tilde{\theta}\,|Q_i| \geq Q_{\min} \\ A_2 \cdot \Delta\tilde{\theta}\,|Q_i| < Q_{\min} \end{cases} \tag{12}$$

TABLE I
SIMULATION PARAMETERS

Symbol	Item	Value
V^*/f_{ref}	Voltage reference	200 V/50 Hz
$P^*_{\max}$	Rated power	10 kW
$Q_{\min}$	Constant reactive power	0.1 kVar
$\Delta\omega_{\max}$	Max frequency deviation	0.5 Hz
K	Controlled coefficient	5e-5
L_{line}	Line inductance	1.8 mH
Z_{load}	Load in t $\in$ [0 s, 1 s]	10 + j5 Ω
	Load in t $\in$ [1 s, 2 s]	10 – j5 Ω

where $A_1 = -M_1 \cdot L$, $A_2 = -M_2 \cdot L$ and L is a Laplacian matrix of a complete graph.

$$\begin{array}{l} \Delta\tilde{\theta} = diag\left[\,\Delta\tilde{\theta}_1\ \Delta\tilde{\theta}_2\ \cdots\ \Delta\tilde{\theta}_n\,\right] \\ M_1 = diag\left(C_1\ C_1\ \cdots\ C_1\right) \\ M_2 = diag\left(C_2\ C_2\ \cdots\ C_2\right) \end{array} \quad L = \begin{bmatrix} n-1 & -1 & \cdots & -1 \\ -1 & n-1 & \cdots & -1 \\ \vdots & \vdots & \ddots & \vdots \\ -1 & -1 & \cdots & n-1 \end{bmatrix}_{n\times n}.$$

From (12), the L is positive semi-definite with eigenvalues $0 = \lambda_1(L) < \lambda_2(L) \leq \cdots \leq \lambda_n(L)$, and the eigenvalue at zero is corresponding to rotational symmetry [13].

Since M_1 and M_2 are scalar matrixes, A_1 and A_2 are also Laplacian matrixes. Thus, all the nonzero eigenvalues of A_i ($i \in \{1, 2\}$) are on the left-half plane, i.e., the system is always stable under both the inductive and capacitive loads. Compared to [10] which is stable only under inductive loads, the proposed method is suitable for wider applications.

It is worth noting that the Laplacian matrix *L* is a complete graph with all the nonzero eigenvalues $\lambda_2(L) = \cdots = \lambda_n(L) = n$ [14]. The eigenvalues of A_i are derived as $\lambda_1(A_i) = 0$ and $\lambda_2(A_i) = \cdots = \lambda_n(A_i) = -n \times C_i$, $i \in \{1, 2\}$. As $\lambda_2(A_i)$ determines the rate of convergence, then with increasing the K, the response speed of proposed control will be improved.

Furthermore, a proper value of $Q_{\min}$ should be selected. To better avoid singularity and guarantee good dynamic performance, $Q_{\min}$ cannot be too small. For simplicity, $Q_{\min}$ could be set to one percent of the rated power of the DG. In fact, the following simulation results also verify this is a simple and practical choice.

III. SIMULATION RESULTS

The simulations are carried out to validate the proposed ideas. The simulation parameters of the system comprised of three cascaded DGs are listed in Table I. There is a small line inductance L_{line} between inverter and load. The control scheme is presented in Fig. 2. The limiter is added to restrict the frequency within the allowable range $f \in (49, 51)$ [15].

1) *Case I: Simulation results of proposed control under both resistive-inductive and resistive-capacitive loads.*

The simulation results are shown in Fig. 3 under both resistive-inductive and resistive-capacitive loads. To illustrate the effectiveness, the different initial phase angles of converters are set at time 0 s and 1 s, and the proposed control starts at 0.3 s and 1.3 s. From Fig. 3, the system can achieve real-power and reactive-power balance in steady-state and obtain a satisfying transient response.

2) *Case II: Simulation results of adding a small disturbance when* $Q_{1\,s} = Q_{2\,s} = Q_{3\,s} = Q_{\min}$

As each DG is controlled by a switched control law as shown in (5) and (7), the behaviour around the piecewise point: $|Q_i| = Q_{\min}$ is more complex. To study robustness at the piecewise point, we assume that

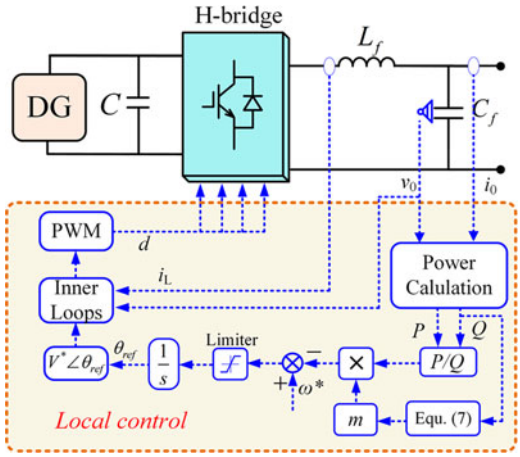

Fig. 2. The local control diagram of the *i-th* DG.

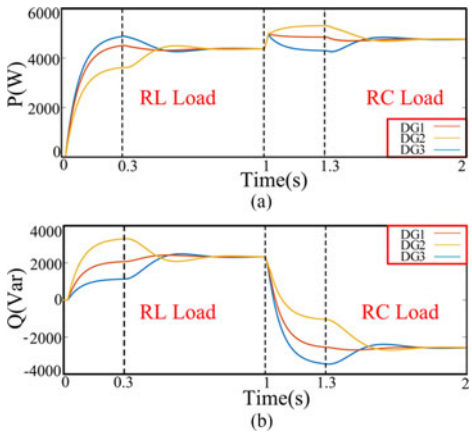

Fig. 3. Simulation results of case I. (a) Active power. (b) Reactive power.

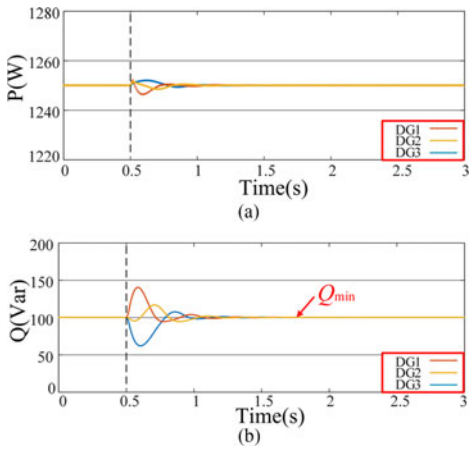

Fig. 4. Simulation results of case II. (a) Active power. (b) Reactive power.

the system is getting into steady state where $Q_{1s} = Q_{2s} = Q_{3s} = Q_{\min} = 100$ Var and $P_{1s} = P_{2s} = P_{3s} = 1250$ W. At $t = 0.5$ s, a small frequency disturbance is added.

From the simulation results in Fig. 4, although the steady state is broken at $t = 0.5$ s, the deviations of active power and reactive power are gradually reduced and the system returns to steady state finally. Moreover, the steady points remain the same before and after disturbance. The simulation results in case II indicate that the proposed control scheme is robust.

IV. Conclusion

This letter reports an $f - P/Q$ droop control scheme for DGs in the cascaded-type microgrid. It realizes accurate real-power and reactive-power balance under both resistive-inductive and resistive-capacitive loads autonomously. Meanwhile, it is convenient to regulate the ac bus voltage.

References

[1] N. Hatziargyriou, H. Asano, R. Iravani, and C. Marnay, "Microgrids," *IEEE Power Energy Mag.*, vol. 5, no. 4, pp. 78–94, Jul./Aug. 2007.
[2] Y. Sun, X. Hou, J. Yang, H. Han, M. Su, and J. M. Guerrero, "New perspectives on droop control in AC microgrid," *IEEE Trans. Ind. Electron.*, vol. 64, no. 7, pp. 5741–5745, Jul. 2017.
[3] X. Lu, K. Sun, J. M. Guerrero, J. C. Vasquez, and L. Huang, "State-of-Charge balance using adaptive droop control for distributed energy storage systems in DC microgrid applications," *IEEE Trans. Ind. Electron.*, vol. 61, no. 6, pp. 2804–2815, Jun. 2014.
[4] I. U. Nutkani, P. C. Loh, P. Wang, and F. Blaabjerg, "Cost-prioritized droop schemes for autonomous AC microgrids," *IEEE Trans. Power Electron.*, vol. 30, no. 2, pp. 1109–1119, Feb. 2015.
[5] A. Elrayyah, Y. Sozer, and M. Elbuluk, "Microgrid-connected PV-based sources: a novel autonomous control method for maintaining maximum power," *IEEE Ind. Appl. Mag.*, vol. 21, no. 2, pp. 19–29, Mar./Apr. 2015.
[6] H. Akagi, "Classification, terminology, and application of the modular multilevel cascade converter (MMCC)," *IEEE Trans. Power Electron.*, vol. 26, no. 11, pp. 3119–3130, Nov. 2011.
[7] S. B. Kjaer, J. K. Pedersen, and F. Blaabjerg, "A review of single-phase grid-connected inverters for photovoltaic modules," *IEEE Trans. Ind. Appl.*, vol. 41, no. 5, pp. 1292–1306, Sep./Oct. 2005.
[8] L. Maharjan, S. Inoue, H. Akagi, and J. Asakura, "State-of-Charge (SOC)-balancing control of a battery energy storage system based on a cascade PWM converter," *IEEE Trans Power Electron.*, vol. 24, no. 6, pp. 1628–1636, Jun. 2009.
[9] G. Xu, D. Sha, and X. Liao, "Decentralized inverse-droop control for input-series–output-parallel DC–DC converters," *IEEE Trans. Power Electron.*, vol. 30, no. 9, pp. 4621–4625, Sep. 2015.
[10] J. He, Y. Li, B. Liang, and C. Wang, "Inverse power factor droop control for decentralized power sharing in series-connected micro-converters based islanding microgrids," *IEEE Trans. Ind. Electron.*, vol. 64, no. 9, pp. 7444–7454, Sep. 2017.
[11] E. A. A. Coelho, P. C. Cortizo, and P. F. D. Garcia, "Small-signal stability for parallel-connected inverters in stand-alone AC supply systems," *IEEE Trans. Ind. Appl.*, vol. 38, no. 2, pp. 533–542, Mar./Apr. 2002.
[12] M. Debasish. *Power System Small Signal Stability Analysis and Control*. New York, NY, USA: Academic, 2014, ch. 5, pp. 119–143.
[13] J. W. Simpson-Porco, F. Dörfler, and F. Bullo, "Synchronization and power sharing for droop-controlled inverters in islanded microgrids," *Automatica*, vol. 49, no. 9, pp. 2603–2611, May. 2012.
[14] F. L. Lewis, H. Zhang, and K. Hengster-Movric, *Cooperative Control of Multi-Agent Systems: Optimal and Adaptive Design Approaches*. New York, NY, USA: Springer, 2014.
[15] I. U. Nutkani, P. C. Loh, P. Wang, and F. Blaabjerg, "Decentralized economic dispatch scheme with online power reserve for microgrids," *IEEE Trans. Smart Grid*, vol. 8, no. 1, pp. 139–148, Jan. 2017.